Inward Transport and Compression of a Positron Plasma by a Rotating Electric Field

R. G. Greaves[1] and C. M. Surko[2]

[1]*First Point Scientific, Inc., 5330 Derry Avenue, Suite J, Agoura Hills, California 91301*
[2]*Department of Physics, University of California, San Diego, California 92093-0319*
(Received 8 May 2000)

Inward transport of a magnetized pure positron plasma confined in a Penning-Malmberg trap is produced by applying a rotating electric field to the plasma. Compression is observed over a broad range of frequencies. Compression factors up to 20 in central density were obtained. Positron collisions with a neutral buffer gas are used to counteract the heating due to the rotating electric field. The results have implications for a variety of applications including the production of brightness enhanced positron beams, the study of electron-positron plasmas, and antihydrogen production.

PACS numbers: 52.25.Wz, 52.25.Fi

Techniques to cool and manipulate low-energy positrons have found application in areas as diverse as atomic physics [1], materials and surface science [2], plasma physics [3], mass spectrometry [4], and astrophysical simulations [5]. The ability to accumulate positrons in Penning traps has extended many of these applications and led to new ones [6]. A recent outgrowth of positron trapping has been the extraction of high quality pulsed beams with energy spreads as low as 18 meV [7], while cooling of positrons using laser-cooled ions has the potential to produce subkelvin beams [8].

One capability of trap-based beams is the potential for brightness enhancement by compression of the positron plasma prior to beam extraction. Other applications of this compression technique include long-term storage of antimatter, the creation of high density positron plasmas for electron-positron plasma experiments [3], antihydrogen formation [9], and the cooling of highly charged ions [10]. In this Letter, we present the first experimental demonstration of radial compression of a positron plasma by the application of a rotating electric field. Inelastic collisions with a low-pressure buffer gas provided the required cooling.

Experiments of this type are also of relevance in understanding how waves and electric fields alter the transport properties of magnetized plasmas. These processes are believed to dominate anomalous transport in a variety of magnetically confined neutral plasmas [11], and their study in the unusually simple geometry of the single component plasma has the potential for yielding new insights [12].

One method of compressing non-neutral plasmas is to vary the plasma rotation frequency using radiation pressure from laser beams [13]. This technique, however, is restricted to certain species of ion plasmas. A more general method that can also be applied to other types of non-neutral plasmas is the injection of angular momentum by exciting plasma waves that rotate faster than the plasma column. Compression of both electron and ion non-neutral plasmas has already been demonstrated using this technique by applying a rotating electric field. In ion plas-

mas, the signal is applied at a frequency slightly above the $E \times B$ rotation frequency of the plasma [14]. For crystallized ion plasmas, the rotation frequency can be phase locked to the applied frequency [15]. In electron plasmas the frequencies employed are somewhat above the rotation frequency. Maximal plasma compression was obtained when the applied frequencies coincided with those of rotating Trivelpiece-Gould (TG) modes [16–18].

In both cases, a strong cooling mechanism was required to counteract the heating produced by the applied rotating electric field. In the ion plasma experiments, laser cooling or neutral gas cooling was employed. Early electron plasma experiments demonstrated the ability to produce inward transport by a rotating field but achieved only modest compression because of strong heating [19]. Other experiments utilized this heating to replenish the plasma by ionization [20]. More recent electron plasma experiments used cyclotron cooling in the strong magnetic field of a superconducting magnet [16,21]. For many positron applications it is desirable to avoid a strong magnetic field, especially if positrons must be extracted into the electrostatic beam lines that, for example, could be used for materials science studies and atomic physics experiments. Unfortunately, in a low magnetic field the cyclotron cooling is slow, and so an alternative mechanism must be sought. For the experiments presented here, cooling by positron collisions with a neutral buffer gas was employed.

The ideal cooling gas for positrons should have a low annihilation cross section, large cross sections for inelastic processes such as vibrational and rotational excitation, and a low elastic collision cross section to avoid enhancing cross-field transport. Unfortunately, very little is known about positron-molecule collision cross sections in the energy regime of interest (i.e., <1 eV). On the basis of the above criteria, the following gases were chosen for study: N_2, CF_4, SF_6, CO_2, and CO.

The compression experiments were performed in the cylindrical Penning-Malmberg trap illustrated in Fig. 1. The trap consists of four cylindrical electrodes of length 3.8 cm and inner diameter 2.54 cm. The electrode S_2 is azimuthally segmented to allow the application of an
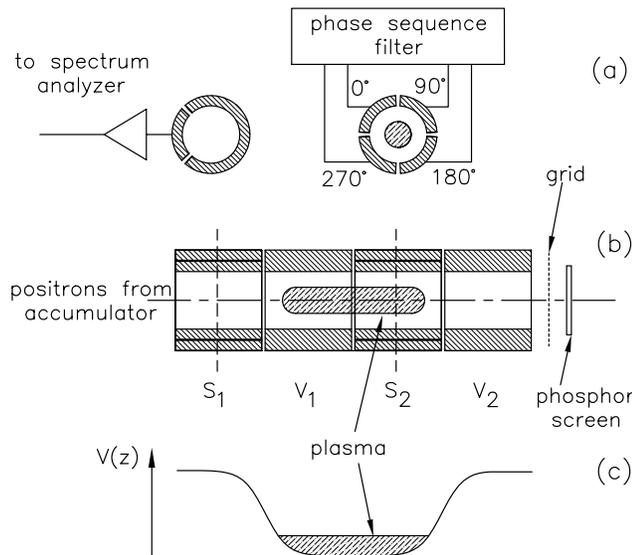
FIG. 1. (a) Electrical connections to segmented electrodes. (b) Layout of the positron trap used for compression experiments. (c) Axial potential well.

$m_\theta = 1$ azimuthal perturbation, and S_1 is segmented as shown in Fig. 1 to measure oscillations excited in the plasma. The excitation field consisted of four sine waves of amplitude A_w and frequency f_w, with relative phases shifted by 90° generated by a broadband phase shifter (0.1–4 MHz). The trap is housed in a vacuum chamber pumped to a base pressure $\sim 1 \times 10^{-9}$ torr. The radial profiles of the plasma are measured by dumping the positrons from the trap onto a phosphor screen biased to -8 kV and imaging the screen using a CCD camera.

Typical parameters before compression were magnetic field, $B = 900$ G, plasma length, $L_p = 6$ cm, plasma radius, $R_p = 3.3$ mm, number of positrons $N_{\text{tot}} = 1 \times 10^7$, average positron density $n_0 = 5 \times 10^6$ cm^{-3}, plasma frequency, $\omega_p/2\pi = 20$ MHz, rotation frequency, $\omega_r/2\pi = 50$ kHz, plasma temperature, $k_B T_p = 0.025$ eV, and Debye length, $\lambda_D = 0.5$ mm. From these parameters, it can be seen that $\lambda_D \ll L_p, R_p$ and $n_0 \lambda_D^3 \sim 10^3 \gg 1$, so the positron cloud is in a well-defined plasma state. In the compressed state, $R_p \simeq 0.7$ mm, yielding $n_0 = 8 \times 10^7$ cm^{-3}.

Positrons were obtained from the third stage of a separate three-stage positron trap that accumulates positrons from a radioactive source [6,22]. Cooling rates were measured by filling the third stage of the trap for a time short compared to cooling times of the respective gases (~ 10 ms) and then by releasing the positrons from the trap after a variable delay. When initially trapped, positrons have a residual energy of several eV from the injection process. The positrons cool to room temperature by collisions with gas molecules. By measuring the number of positrons released from the trap as a function of the exit gate potential, the positron temperature can be obtained. By using this technique, the cooling times were measured

for the selected gases. The results are presented in Table I, together with other parameters relevant to this experiment. These data indicate that cooling times comparable to those of cyclotron radiation cooled plasmas in the field of a superconducting magnet can be obtained using gas cooling at pressures as low as 2×10^{-8} torr, where positron annihilation is negligible.

For compression experiments, positrons were transferred from the three-stage accumulation trap to the compression trap. Compression was studied by applying a fixed frequency to the plasma and then dumping the plasma onto the phosphor screen. Data thus obtained, showing rapid compression of a positron plasma, are presented in Fig. 2(a). Because the transport is rapid, the plasma does not evolve to an equilibrium profile while the transport is occurring, but, rather, it immediately develops a dense core which grows in time as the surrounding plasma is driven inward. When the signal was applied to the entire length of the plasma (using electrode V_1 and V2 as the end electrodes), no compression was observed. There is very little loss of positrons ($<5\%$) during compression.

Figure 2(b) shows the time dependence of the central plasma density for different amplitudes of the applied signal. If no signal is applied, the central density decays with an exponential time constant ~ 11 s. If even a small rotating electric field is applied (~ 2 mV), this outward diffusion is reversed, and for larger amplitudes strong inward transport is obtained. (If the direction of rotation is reversed, the plasma is driven rapidly out to the wall.) Initially there is an approximately linear increase of density, followed by a nonlinear phase and eventual saturation. The minimum radius does not show a strong dependence on the number of positrons in the trap. The smallest radius that was observed was $R_p \simeq 0.7$ mm, with an increase of 20 in central density. Factors determining the minimum radius are not understood at present, but a small $m = 1$ diocotron mode that is observed to grow as the plasma is compressed may play a determining role. The observed compression rates are about a factor of 30 larger than those reported in the experiment of Anderegg et al. [16]. Attempts to directly detect the excitation of plasma modes using the pickup electrode failed.

TABLE I. Parameters for cooling gases at 2×10^{-8} torr: annihilation time τ_a (from Ref. [23]), measured cooling time τ_c, vibrational quanta E_ν, relevant to the cooling, where known, and maximum measured compression rate $\dot{n}/n_{\text{max}}$.

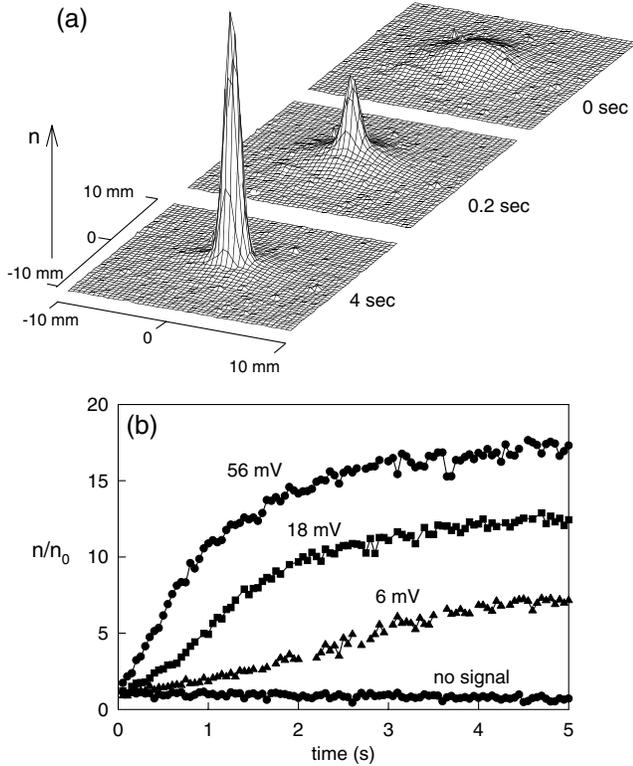| Gas	$\tau_a(s)$	$\tau_c(s)$	E_ν (eV)	$\dot{n}/n_{\text{max}}$ (s^{-1})
SF_6	2190	0.36	–	10
CF_4	3500	1.2	0.157	10
CO_2	3500	1.3	0.291, 0.083	4
CO	2400	2.1	0.266	<0.2
N_2	6300	115	0.292 eV	<0.2

FIG. 2.   (a) Radial profiles of a positron plasma with $N_{tot} = 10^7$ positrons, $f_w = 2.5$ MHz, $A_w = 56$ mV, and 2×10^{-8} torr of CF_4.   (b) Time evolution of the central density, normalized to its initial value for various values of the applied amplitude.

FIG. 3.   Positron density after 1 s of compression for ($\circ$) $N_{tot} = 1 \times 10^7$ positrons and ($\bullet$) $N_{tot} = 5 \times 10^6$ positrons with 2×10^{-8} torr CF_4: (a) Frequency dependence for $A_w = 56$ mV. Arrows indicate the frequencies for the lowest order TG modes for the initial plasma conditions. (b) Amplitude dependence for $f_w = 2.5$ MHz.

In Fig. 3, data are presented for the dependence of compression on the frequency and amplitude of the applied signal. The data in Fig. 3(a) were obtained with frequencies in the range 0.1–4 MHz and $A_w = 56$ mV applied for 1 s. The central density is normalized to the initial value. For comparison with earlier experiments, we calculated the mode frequencies for the lowest order TG modes. For the relevant limit, $kR_p \ll 1$, the dispersion relation for the TG modes with $m_\theta = 1$ and radial mode number l is $\omega \simeq \omega_r \pm kR_p \omega_p / p_l$, where p_l is the lth root of $J_1(x) = 0$ [17]. The frequencies f_1 and f_2 of the two lowest-order modes with $m_z = 1$ and $m_z = 2$, respectively, are indicated by arrows in Fig. 3(a). It can be seen that compression is observed for frequencies in the range of these low-order TG modes. It is interesting to note, however, that the effect is broadband in character, in contrast to the resonances reported in Ref. [16].

Figure 3(b) shows data for compression as a function of the amplitude of the applied signal. The quantity $\Delta n / n_0$ is plotted, where Δn is the increment in central density after 1 s and n_0 is the initial value. For the lower amplitudes, this is a reasonable approximation to the compression rate $\dot{n}/n$. The initial compression rate follows the predictions of linear theory, i.e., $\dot{n}/n \propto A_w^2$ [16]. Thereafter, the compre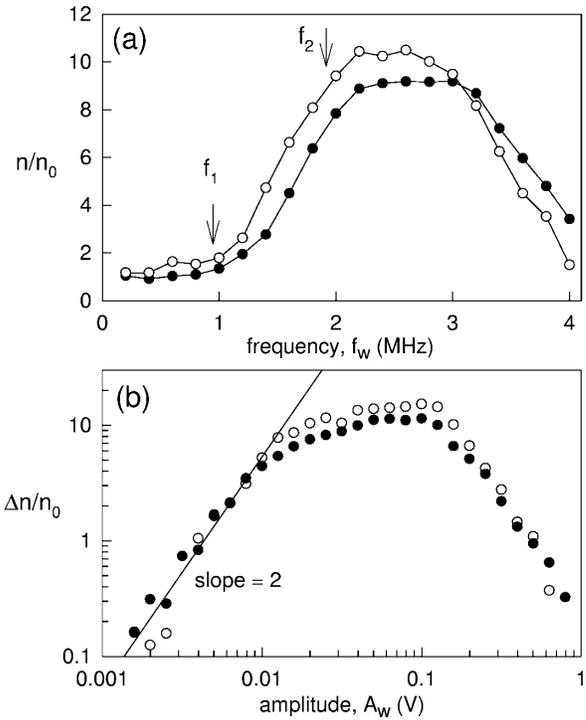ssion rate begins to level off until some critical amplitude, after which it drops off as the amplitude is further increased.

Figure 4 shows the effect of varying the cooling gas pressure. No significant compression is observed in the absence of a cooling gas. For $P = 2 \times 10^{-8}$ torr, substantial compression is observed. If the pressure is doubled, there is no significant effect on the compression rate for low drive amplitudes, but at high amplitudes (in the nonlinear regime) the compression effect is increased, although it does not scale linearly with pressure. These data show clearly the crucial role played by the cooling gas.
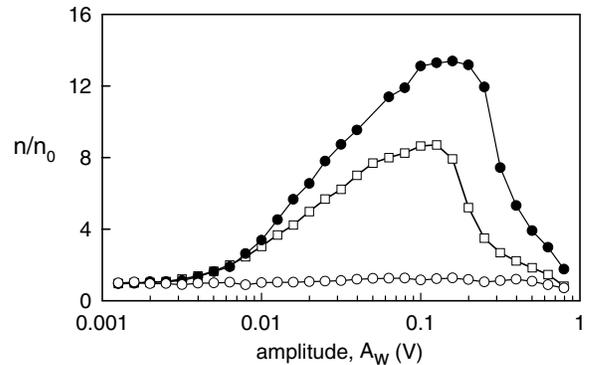

FIG. 4.   Compression for cooling on CF_4 with $N_{tot} = 5 \times 10^6$ positrons and $f_w = 2.5$ MHz for 1 s: ($\bullet$) $P = 4 \times 10^{-8}$ torr; ($\square$) $P = 2 \times 10^{-8}$ torr; ($\circ$) no cooling gas.

We have also studied the effect of different gases. In general, they exhibit behavior similar to Fig. 4, but produce different compression rates, which are summarized in Table I. One surprising result is the low compression obtained when using CO, which has a relatively high cooling rate. This shows that complicating factors play a role in the cooling process, probably reflecting details of the energy dependence of the positron-molecule cross sections. For example, CO has one of the largest vibrational quanta of the gases studied (see Table I), resulting in less effective cooling below this energy.

There are a number of interesting similarities and differences from the earlier electron plasma studies. These differences can be understood qualitatively in terms of the differences in the plasma parameters and, in particular, the damping rates. The damping rate, γ, scales as $\gamma/\omega \sim -(1/2)(v_\phi/v_{th})^3 \exp[-(v_\phi/v_{th})^2/2]$, where $v_\phi \sim (\omega - m_\theta \omega_r)/k$ is the wave phase velocity and v_{th} is the positron thermal velocity [18]. For the earlier experiment, $\gamma/\omega \sim -0.01$, while, for the present experiment, $\gamma/\omega \sim -0.6$. The much stronger damping in the present experiment can account qualitatively both for the higher compression rates (because of the more direct coupling between the applied electric field and particles) and for the nonresonant nature of the interaction, due to mode broadening. It also accounts for the failure to observe the mode directly on the pickup electrodes. The strong damping may also explain the scaling $\dot{n}/n \propto A_w^2$ observed here but not in previous experiments. The present experimental results are therefore consistent with the excitation of TG modes, as reported by Anderegg *et al.* [16].

The results presented here have implications for a range of low-energy positron applications. One application is the production of brightness enhanced positron beams for positron microscopy and other uses. Currently, such beams are produced by using the technique of remoderation brightness enhancement [24]. By using positron plasma compression, it is, in principle, possible to achieve the same effect with much higher efficiencies. This technique also has practical implications for the manipulation of positrons in other areas of research where high density positron plasmas are desirable. These include the production of antihydrogen [9], the cooling of highly charged ions [10], electron-positron plasma experiments [3], and mass spectrometry [4].

In summary, we have made the first experimental demonstration of compression of a magnetized positron plasma by applying a rotating electric field at frequencies well above the rotation frequency. A key element of these experiments was the implementation of buffer gas cooling using suitably chosen polyatomic gases.

[1] W. E. Kauppila and T. S. Stein, Adv. At. Mol. Opt. Phys. **26**, 1 (1990).

[2] P. J. Schultz and K. G. Lynn, Rev. Mod. Phys. **60**, 701 (1988).

[3] R. G. Greaves and C. M. Surko, Phys. Rev. Lett. **75**, 3846 (1995).

[4] L. D. Hulett Jr., *et al.,* Chem. Phys. Lett. **216**, 236 (1993).

[5] B. L. Brown, M. Leventhal, A. P. Mills, Jr., and D. W. Gidley, Phys. Rev. Lett. **53**, 2347 (1984).

[6] R. G. Greaves and C. M. Surko, Phys. Plasmas **4**, 1528 (1997).

[7] S. J. Gilbert, C. Kurz, R. G. Greaves, and C. M. Surko, Appl. Phys. Lett. **70**, 1944 (1997).

[8] D. J. Wineland, C. S. Weimer, and J. J. Bollinger, Hyperfine Interact. **76**, 115 (1993).

[9] M. Charlton *et al.,* Phys. Rep. **241**, 65 (1994).

[10] D. A. Church, Phys. Scr. **46**, 278 (1992).

[11] B. A. Carreras, IEEE Trans. Plasma Sci. **25**, 1281 (1997).

[12] D. L. Eggleston, T. M. O'Neil, and J. H. Malmberg, Phys. Rev. Lett. **53**, 982 (1984).

[13] J. J. Bollinger and D. J. Wineland, Phys. Rev. Lett. **53**, 348 (1984); D. J. Heinzen *et al.,* Phys. Rev. Lett. **66**, 2080 (1991).

[14] X.-P. Huang *et al.,* Phys. Rev. Lett. **78**, 875 (1997).

[15] X.-P. Huang *et al.,* Phys. Rev. Lett. **80**, 73 (1998).

[16] F. Anderegg, E. M. Hollmann, and C. F. Driscoll, Phys. Rev. Lett. **81**, 4875 (1998).

[17] R. W. Gould, in *Non-neutral Plasma Physics III,* edited by J. J. Bollinger, R. L. Spencer, and R. C. Davidson, AIP Conf. Proc. No. 498 (AIP, New York, 1999), p. 170.

[18] E. M. Hollmann, F. Anderegg, and C. F. Driscoll, Phys. Plasmas (to be published).

[19] T. B. Mitchell, Ph.D. thesis, University of California, San Diego, 1993.

[20] R. E. Pollock and F. Anderegg, in *Non-Neutral Plasma Physics II,* edited by J. Fajans and D. H. E. Dubin, AIP Conf. Proc. No. 331 (AIP, New York, 1995), p. 139.

[21] T. Ichioka *et al.,* in *Non-neutral Plasma Physics III* (Ref. [17]), p. 59.

[22] C. M. Surko, M. Leventhal, and A. Passner, Phys. Rev. Lett. **62**, 901 (1989).

[23] K. Iwata *et al.,* Phys. Rev. A **51**, 473 (1995).

[24] A. P. Mills, Jr., Appl. Phys. **23**, 189 (1980).